Progress In Electromagnetics Research C, Vol. 112, 139–151, 2021

Circularly Polarized Multiple Layer Dielectric Resonator Antennas

Richa Gupta[1, *], Ankit Gaur[2], Sandeep Gupta[3], and Garima Bakshi[4]

Abstract—A sequence of anisotropic and isotropic materials of dielectric constant 12 and 10 respectively have been stacked alternatively to form a four-layer stack structure with aperture coupled feed mechanism for excitation. Applying this excitation, orthogonal mode pair $TE^{x}_{\delta 21}$ and $TE^{y}_{2\delta 1}$ has been excited at frequencies 7.54 GHz and 7.8 GHz, respectively in YZ and ZX planes to generate circular polarization. A circularly polarized bandwidth in the region (7.54 GHz–7.92 GHz) in conjunction with impedance bandwidth in the region (5.23 GHz–5.52 GHz) with a gain of 5.2 dBi has been accomplished. The designed antenna is appropriate for C-band and weather radar applications. The design assessment has been done using Ansys HFSS. The three stages of antenna design are examined. Further, the design is investigated with a 6-layer structure and an 8-layer structure.

1. INTRODUCTION

The fields of dielectric resonator antennas (DRAs) have been progressing immensely because of their pluses over conventional antennas such as wider bandwidth, radiation efficiency, and evasion of surface waves. The ever-increasing challenge in the world of wireless communication has led to the design and development of such antennas that can offer multifunctionality with maximum advantages at minimum cost and compact design. Since dielectric resonator antennas have come into the picture, only linearly polarized (LP) DRAs have been explored and operated in depth. In recent times, LP-DRAs are seen to be blended with many losses and multipath interface. These shortcomings of LP-DRA have laid path to the effort in the direction of circularly polarized (CP) DRA. CP-DRA has potential to surmount all the downsides of LP-DRA. It also overpowers the effect on the orientation of transmitting and receiving antennas [1–3]. Most of the circularly polarized antenna have dual-feeding mechanism which increases the size and complexity of the circuit. Numerous procedures like generation of higher order modes to generate circular polarisation [4] have been considered in literature to overcome the need of multiple feeds. Practices like altering the shape of DRA are also used to produce circular polarization. Various geometries like trapezoidal-shaped DR [5], zonal slot/DRA [6], stair shape slot DRA [7], and triangular ring shape aperture [8] are considered to accomplish circular polarization. The difficulty in a design adds to the complexity in manufacture process. Stacked antenna structure can be used to enhance gain [9, 10]. Circular polarization is also achieved through structures discussed in [11–14] and cross slot DRA [15]. Generally, DRA is produced from plastic material like polyvinyl chloride (PVC). The antenna created from this stuff is not appropriate for robust and extended-distance communication applications and consequently requests the need of new tough materials to connect the later generation antenna commitments. Hence, sapphire, being stable, can be used [16]. It has a number of benefits such as light transmission characteristics and thermal insulation. As per the Literature assessment very few works have been done employing anisotropic material [17, 18].

It is the latent option for upcoming smart phones and mobile communication.

Received 27 November 2020, Accepted 8 April 2021, Scheduled 4 May 2021

* Corresponding author: Richa Gupta (richagupta@msit.in).

[1,2] Maharaja Surajmal Institute of Technology, Delhi, India. [3] JECRC University Jaipur, Rajasthan, India. [4] School of Engineering & Technology, Ansal University, Gurgaon, India.

A sequence of anisotropic and isotropic materials of dielectric constant 12 and 10 respectively have been stacked

In this document, a design of multiband DRA consisting of anisotropic materials of dielectric constants 12 and 10, respectively, which are stacked alternatively to form a four-layer stack structure, is proposed with aperture coupled feed mechanism for excitation has been presented. The literature indicates that analysis of isotropic DRA has been done intensively as compared to anisotropic material.

The paper further talks about the antenna structure and design in Section 2, supported by an explanation on different designs in Section 3. Further, Sections 4 and 5 examine results along with a parametric study in Section 6. Section 7 presents the conclusion.

2. ANTENNA STRUCTURE AND DESIGN

Figure 1 shows the proposed Rectangular DRA (RDRA). The dielectric resonator structure has been placed on a rectangular FR-4 epoxy substrate having length and width measurements 50 mm × 50 mm along with the thickness of 0.8 mm and dielectric constant of 4.4. Anisotropic material of size 10 mm × 13 mm × 2.5 mm and isotropic material of size 8 mm × 12 mm × 2.5 mm are placed alternatively to form a four-layer layout. The dielectric constants of alternate material are 12 and 10 correspondingly. In addition to this, a patch of size 40 mm × 20 mm with corners trimmed and a cross-slot of dimensions (10 mm × 2.6 mm) cut have been positioned to achieve circular polarization. The method used to excite the antenna structure is aperture coupled technique.

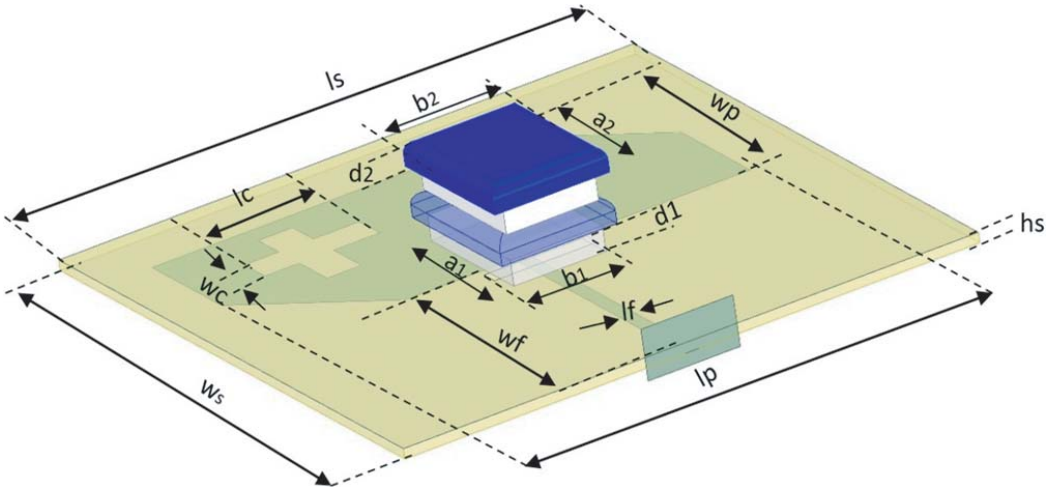

Figure 1. Four layer stacked dielectric resonator (ls = 50 mm; Ws = 50 mm; hs = 0.8 mm; $d1 = d2$ = 2 mm; $a1$ = 8 mm; $a2$ = 10 mm; $b1$ = 12 mmm; $b2$ = 13 mm; lf = 1.2 mm; wc = 2.6 mm; lc = 10 mm; wp = 20 mm; lp = 40 mm; wf = 25 mm.

3. DESIGN PATTERN

Three design configurations are evaluated as shown in Fig. 2. The three are reviewed below. The final design (design 3 as shown in Fig. 2(c)) is endorsed based on improved axial ratio and bandwidth.

Design 1 contains a basic structure that has stacked RDRA, a feedline, and a slot, with specifications of the aperture slot as 1.5 mm × 9 mm and feedline 1.2 mm × 25 mm. This configuration is linearly polarised.

In design 2, all the stacked RDRA parameters are kept constant, and an addition in design is done. Additionally, a patch of dimensions 40 mm × 20 mm has been etched with corner trimmed to provide circular polarisation along with stacked RDRA with feedline and slot. This design change delivers axial ratio less than 3 dB, but less bandwidth is obtained in this design.

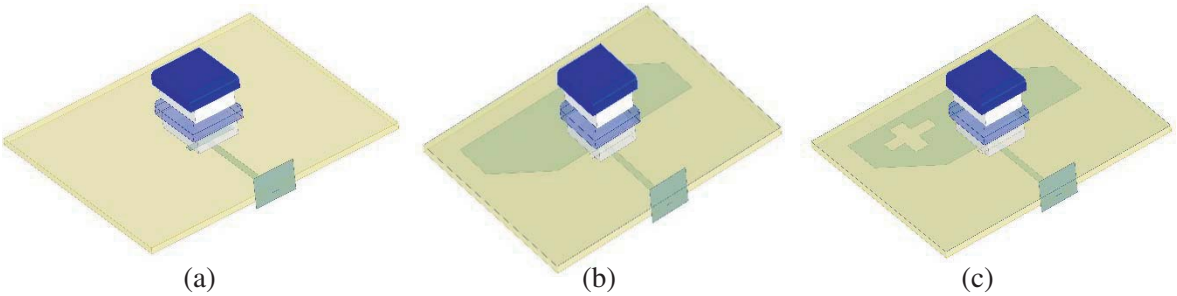

Figure 2. Design of rectangular DRA. (a) Design 1. (b) Design 2. (c) Design 3.

In design 3, which is the final structure design, the structure has been constructed by an extra addition in design 2. Two cross slots of dimension 10 mm × 2.6 are added to it. The insertion of slots results in reducing the quality factor, boosts the response of antenna, and plus consequently improves the bandwidth of antenna.

4. RESULTS AND DISCUSSION

Design 1 does not show any circular polarization. It displays twin 10 dB impedance bandwidths in the frequency regions of (5.29 GHz–5.84 GHz) and (6.92 GHz–7.29 GHz). In design 2, orthogonal mode pair $TE^{x}_{\delta 11}$ and $TE^{y}_{1\delta 1}$ as shown in Fig. 3 has been excited at frequencies 5.95 GHz and 6.05 GHz correspondingly in YZ and XZ planes which is responsible for circular polarization. The E and H plane radiation patterns at frequencies 5.95 GHz and 6.05 GHz are displayed in Fig. 4. Axial ratio is often quoted for antennas in which the desired polarization is circular; however, Axial Ratio: < 3 dB is acceptable. Design 2 bestow three regions of operation (5.26 GHz–5.54 GHz), (6.76 GHz–6.94 GHz), and (7.73 GHz–8.02 GHz). For the frequency range (5.95 GHz–6.05 GHz) at Phi = 0 degrees and theta = 150 degrees, the axial ratio is beneath 3 dB for design 2, displaying circular polarisation.

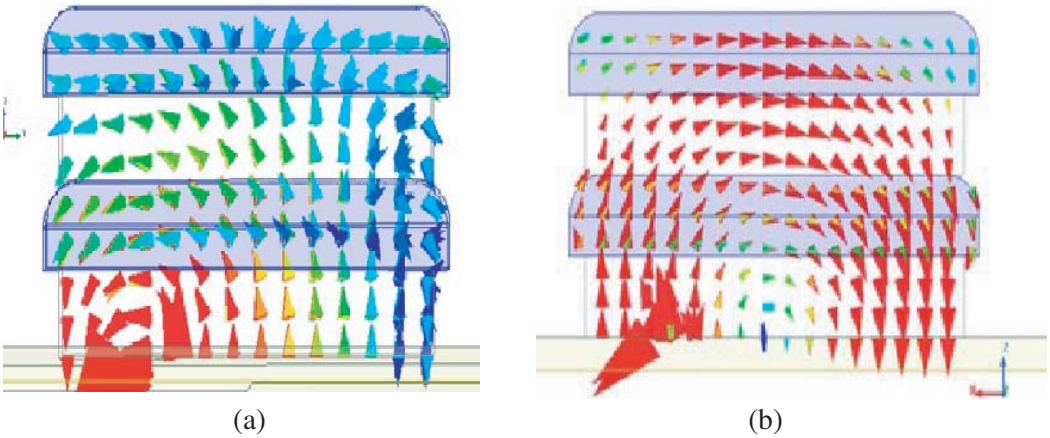

Figure 3. E field distribution of design 2. (a) $TE^{x}_{\delta 11}$ at frequency 5.95 GHz. (b) $TE^{y}_{1\delta 1}$ at frequency 6.05 GHz.

In Fig. 5, S_{11} and axial ratio bandwidth of design 2 are exhibited. At frequency 6 GHz, the LHCP and RHCP radiation patterns at both the planes are shown in Fig. 6. The antenna displays LHCP with cross-polarization separation > 18 dB, which is reasonable for workable application.

In design 2, the antenna was examined lacking of slot. The addition of the slot in design 3 lowers the quality factor, boosts the response of the antenna, and consequently improves the bandwidth of design 3 [19–21]. The field distribution at various resonating frequencies and generation of orthogonal

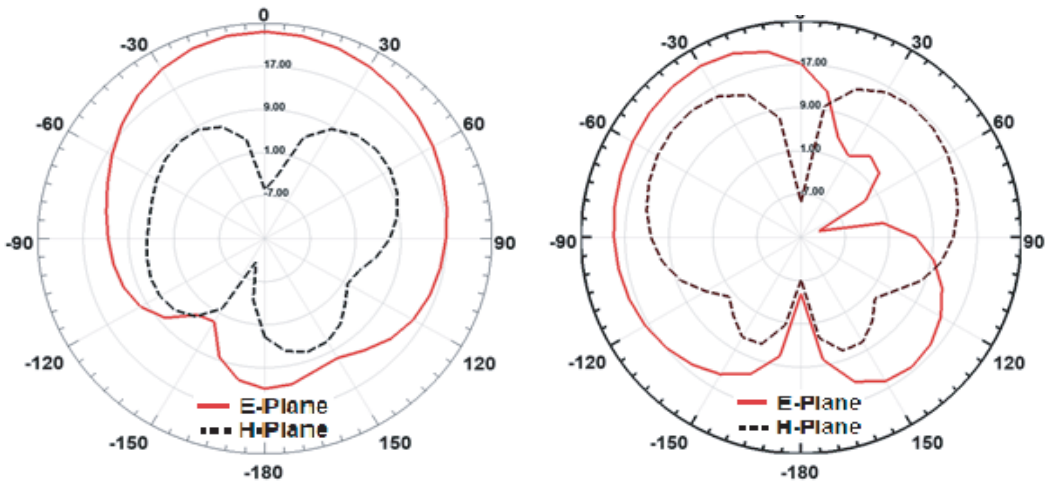

Figure 4. Radiation pattern (design 2) at frequency (a) 5.95 GHz, (b) 6.05 GHz.

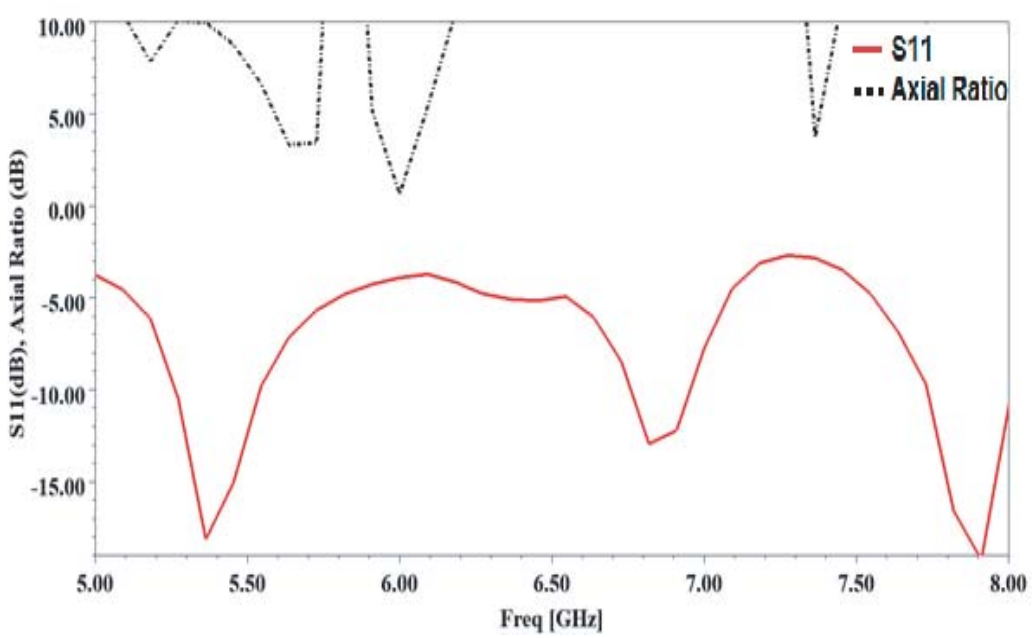

Figure 5. S_{11} and axial ratio bandwidth of design 2.

mode $\mathrm{TE}^{x}_{\delta 21}$ and $\mathrm{TE}^{y}_{2\delta 1}$ at frequencies 7.54 GHz and 7.8 GHz respectively in YZ and XZ planes are displayed in Fig. 7. The impedance and axial ratio bandwidth of design 3 are displayed in Fig. 9. In this configuration, for the frequency range (7.54 GHz–7.92 GHz) axial ratio is below 3 dB at Phi = 0 degrees and theta 100 degrees. The E and H plane variations of radiation patterns at frequency 5.36 GHz and 7.6 GHz are exhibited in Fig. 8. At frequencies 7.6 GHz and 7.9 GHz, the LHCP and RHCP radiation patterns are demonstrated in Fig. 10. It shows that the antenna exhibits RHCP with cross-polarization separation $>$ 18 dB, which is satisfactory for practical application. The gains of three designs is demonstrated in Table 1. All the explored outcomes of three designs are also encapsulated in Table 1. A reasonable analysis of results with other suggested designs is presented in Table 2.

Further, the investigations have been done on stacking materials of dielectric constants 12 and 10 respectively to form six- and eight-layered stacked structures as shown in Figs. 11(a)–(b). As the height of structure increases, higher order modes are generated. The generation of higher order mode $\mathrm{TE}^{x}_{1\&3}$ in

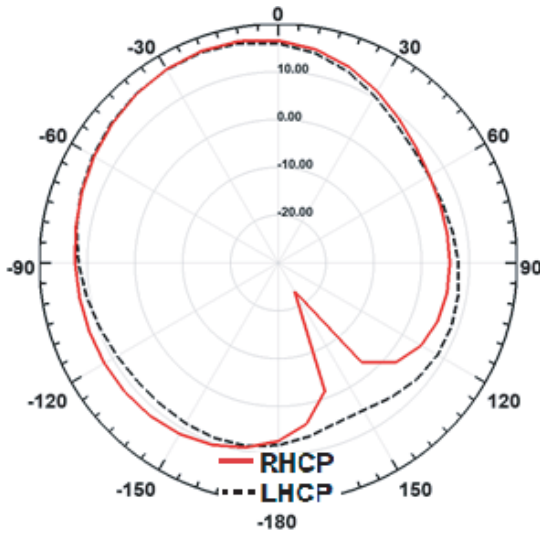

Figure 6. LHCP and RHCP radiation pattern (design 2) at frequency 6 GHz.

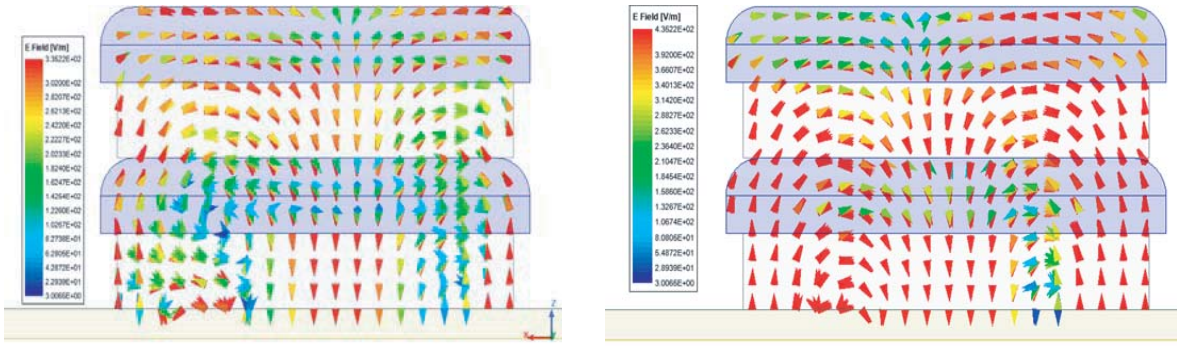

(a) (b)

Figure 7. E field distribution of design 3. (a) $TE^{x}_{\delta 21}$ at frequency 7.54 GHz. (b) $TE^{y}_{2\delta 1}$ at frequency 7.8 GHz.

6 layer stacked DRA and $TE^{x}_{2\delta 3}$ in 8 layer stacked DRA is shown in Figs. 12(a)–(b). The S_{11} responses of three designs, i.e., 4 layers stacked DRA, 6 layers stacked DRA, 8 layers stacked DRA, are shown in Fig. 13. The gain responses of antenna with 4, 6, and 8 stacked layers are demonstrated in Fig. 14. The gain of 8 layered stacked structure is 5.9 dB. The various results are summarized in Table 3.

Table 1. Comparison between various parameters for different design's.

Antenna design	Impedence · BW (GHz)	Axial Ratio BW (GHz)	Gain (dBi)
Design 1	(5.29 GHz–5.84 GHz)	-	5.4
Design 2	(5.26 GHz–5.54 GHz) (6.76 GHz–6.94 GHz) (7.73 GHz–8.02 GHz)	(5.95 GHz–6.05 GHz) 1.66%	5.3
Design 3	(5.23 GHz–5.52 GHz) (7.53 GHz–7.99 GHz)	(7.54 GHz–7.92 GHz) 4.91%	5.2

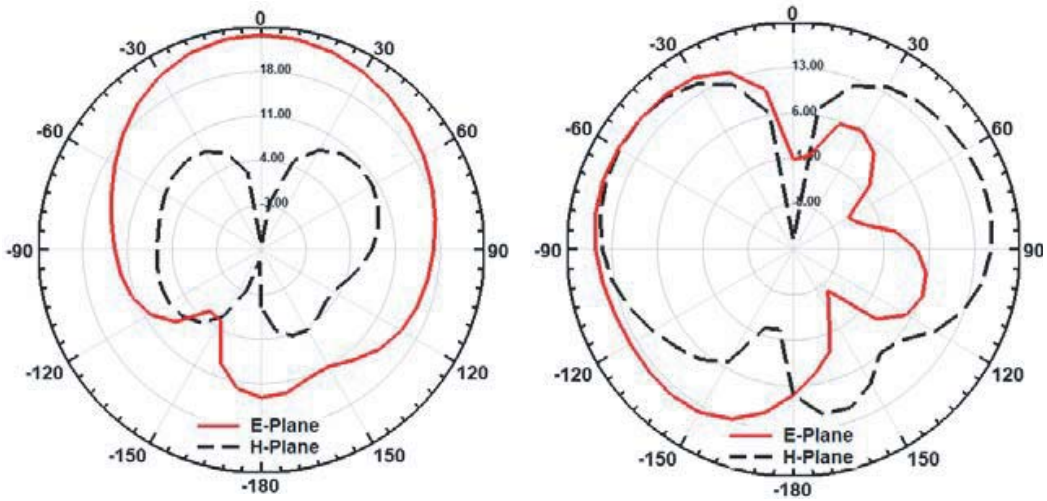

Figure 8. Radiation pattern at frequency (a) 5.36 GHz. (b) 7.6 GHz.

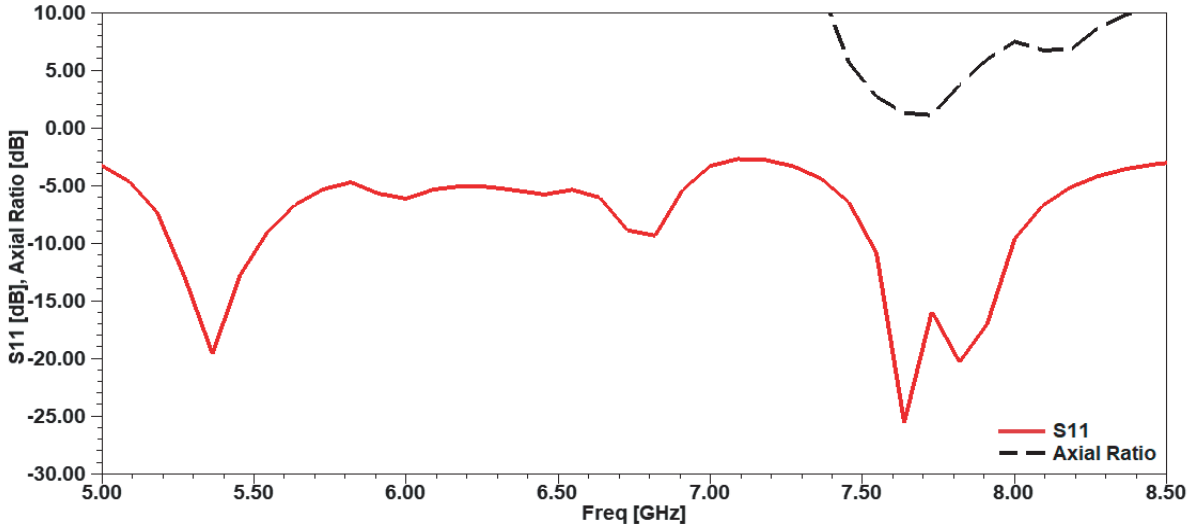

Figure 9. S_{11} and axial ratio bandwidth of design 3.

5. MEASURED RESULTS

The prototype of design 3 under measurement is revealed in Fig. 15. The S_{11} parameter is assessed using a vector network analyzer while axial ratio is measured using the Star Lab system. A closeness between simulated and measured S_{11} is revealed in Fig. 16. The ranges of simulated impedance bandwidths are (5.23 GHz–5.52 GHz) and (7.53 GHz–7.99 GHz), respectively, and the measured impedance bandwidth ranges are (5.27 GHz–5.58 GHz) and (7.29 GHz–7.7 GHz). The simulated and measured axial ratio bandwidth regions of (7.53 GHz–7.99 GHz) and (7.29–7.70 GHz) respectively are displayed in Fig. 17.

6. PARAMETRIC ANALYSIS

To scrutinize optimized execution, a parametric study has been carried out. During the conduction of parametric analysis, one parameter is differed while others are kept steady. The analysis is carried out on two cross slot dimensions. The cross-slot length is diverse from 9.6 mm to 10.2 mm. The impact of

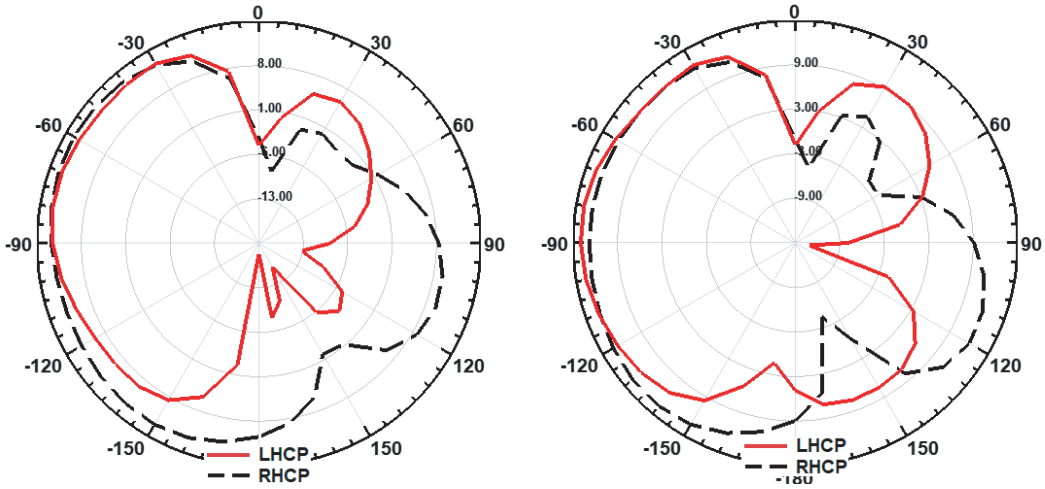

(a) (b)

Figure 10. LHCP and RHCP radiation pattern (design 3) at frequency (a) 7.6 GHz, (b) 7.9 GHz.

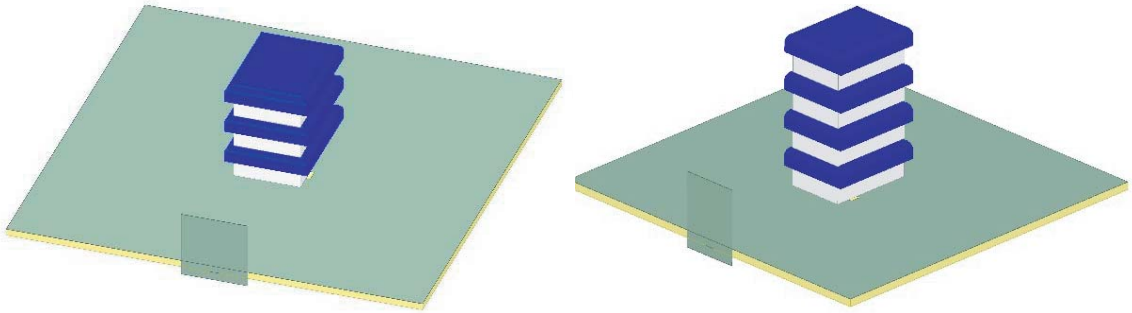

(a) (b)

Figure 11. (a) Design of 6 layer stacked DRA. (b) Design of 8 layered Stacked DRA.

Table 2. Comparison between suggested design with existing design's.

Ref.	Design	Mode	CP Bandwidth	Gain (dBi)
[8]	Triangular Ring shape aperture and parasitic strip Rectangular DRA	$TE^{y}_{1\delta1}$	(3.46 GHz–3.54 GHz) (2.29%)	5
[15]	Cross slot DRA	TE^{y}_{141} and $TE^{y}_{1\delta1}$	(5.18 GHz–5.34 GHz) 3.04%	4.57
[18]	Stacked Open-Loop Square Ring Antenna	-	(2.41 GHz–2.44 GHz) 1.23%	3.7
Proposed DRA	Stacked DRA	$TE^{x}_{\delta21}$ and $TE^{y}_{2\delta1}$	(7.54 GHz–7.92 GHz) 4.91%	5.2

deviations of cross length on S_{11} and axial ratio are validated in Figs. 18(a)–(b). The improved cross slot length is 10 mm.

The evaluation has been carried for cross slot width as indicated in Figs. 19(a)–(b). It has been noticed that impedance bandwidth of antenna remains nearly similar in all cases. Improved axial ratio

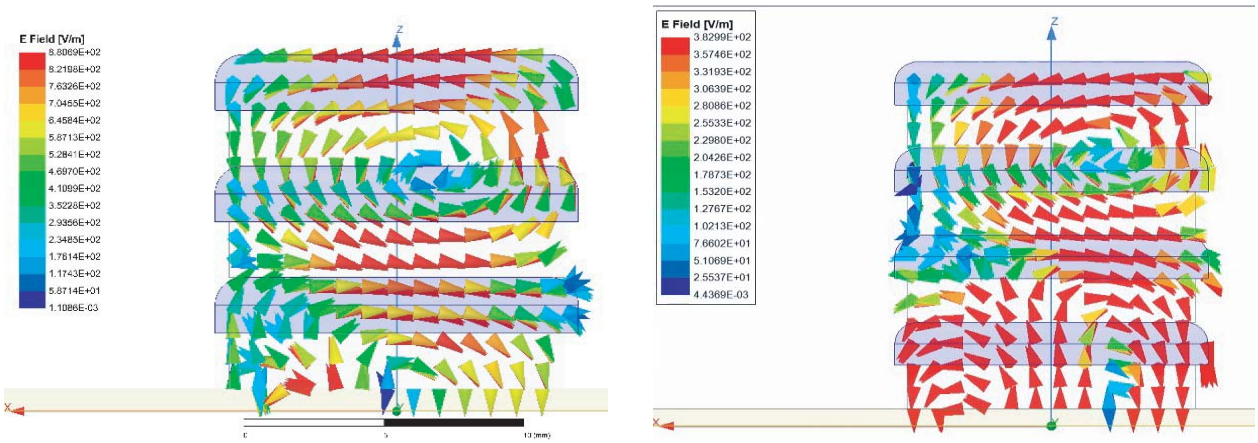

(a) (b)

Figure 12. E field distribution. (a) $\mathrm{TE}^{x}_{1\delta 3}$ at 6 layer stacked DRA; (b) $\mathrm{TE}^{x}_{2\delta 3}$ at 8 layer stacked DRA.

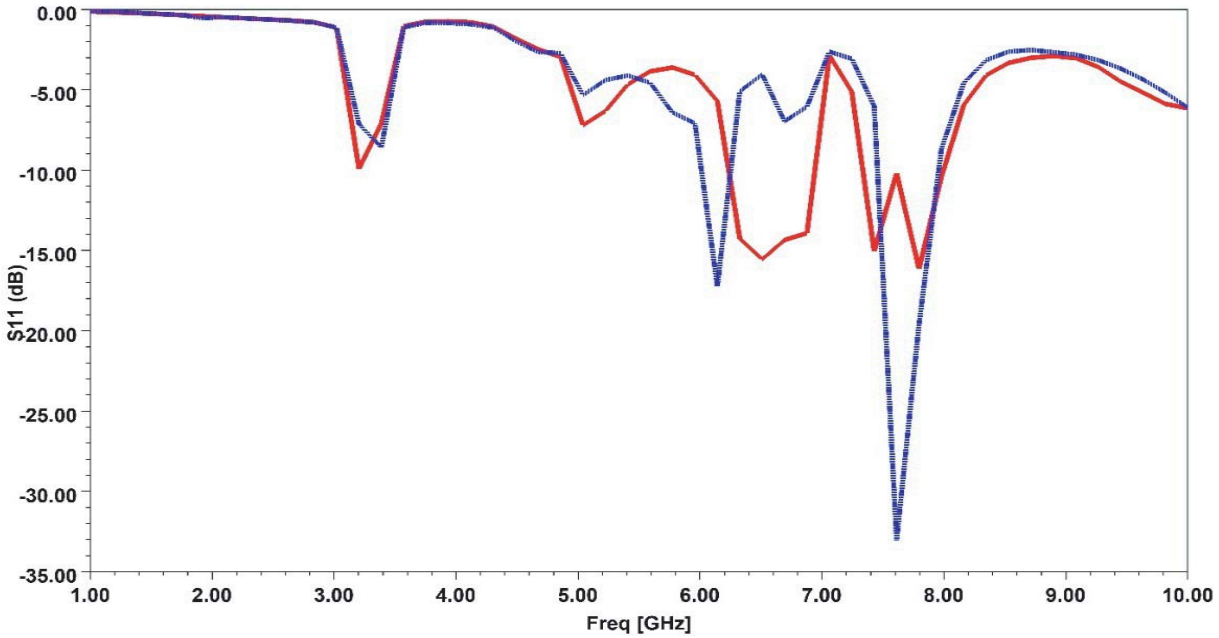

Figure 13. S_{11} of three designs: 6 layers stacked DRA; 8 layers stacked DRA.

Table 3. Comparison between various parameters for 4 layers stacked DRA, 6 layers stacked DRA, 8 layers stacked DRA.

Stacked Structure	Mode	Impedence BW (GHz)	S_{11} (dB)	Gain (dBi)
4 layer	$TE^{x}_{\delta 21}$	(5.23 GHz–5.52 GHz) (7.53 GHz–7.99 GHz)	−26 dB	5.2 dBi
6 layer	$TE^{y}_{1\delta 3}$	(6.24 GHz–6.94 GHz) (7.34 GHz–8.00 GHz)	−16 dB	5.7 dBi
8 layer	$TE^{y}_{2\delta 3}$	(6.01 GHz-6.25 GHz) (7.46 GHz-7.96 GHz)	−34 dB	5.9 dBi

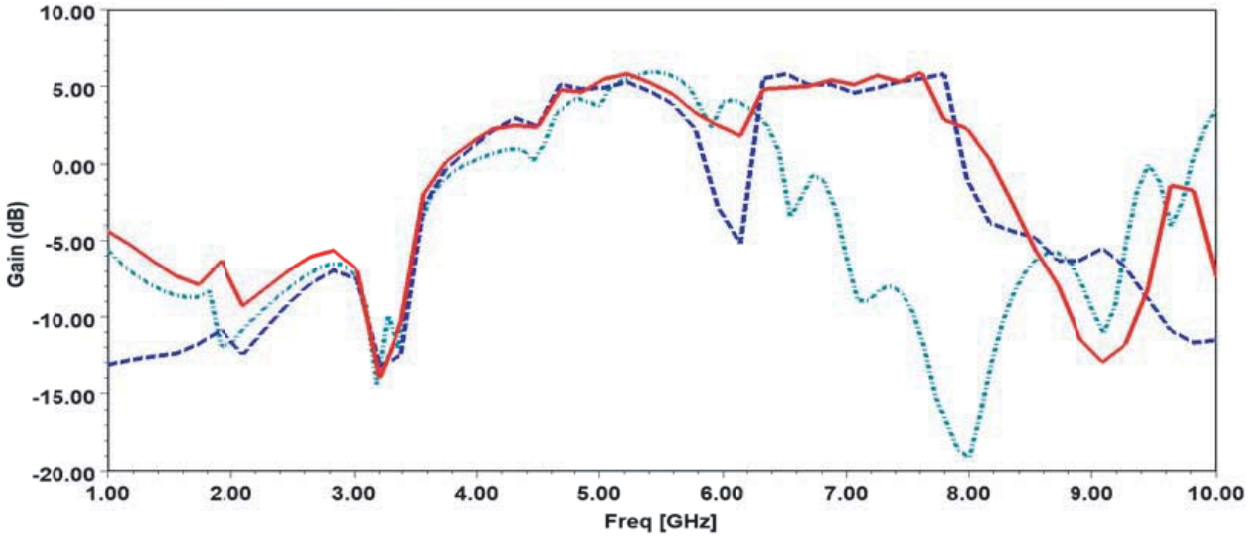

Figure 14. Gain of three designs: 4 layers stacked DRA, 6 layers stacked DRA, 8 layers stacked DRA.

Figure 15. Experimental setup of the prototype.

bandwidth is acquired at 2.6 mm. Further, the assessment has been accomplished for aperture slot length. The aperture slot length is differed from 8.7 mm to 9.3 mm. The impact of modification of length on S_{11} and axial ratio is exhibited in Figs. 20(a)–(b). The optimized length is 9 mm. The evaluation has been conducted for aperture slot widths 1.4 mm, 1.5 mm, and 1.6 mm as displayed in Figs. 21(a)–(b). It has been observed that the impedance bandwidth of antenna remains nearly the same in all cases. The parametric analysis on the increasing height of 6 layered stacked geometry shown in Fig. 11(a) has been performed. The height of the uppermost 6th layer is varied from 2 mm to 2.6 mm. Not much variation in operating frequency bands is observed, but S_{11} becomes better at height of 2.6 mm. The slight increase in gain is observed as the height increases. The results are demonstrated in Figs. 22(a)–(b).

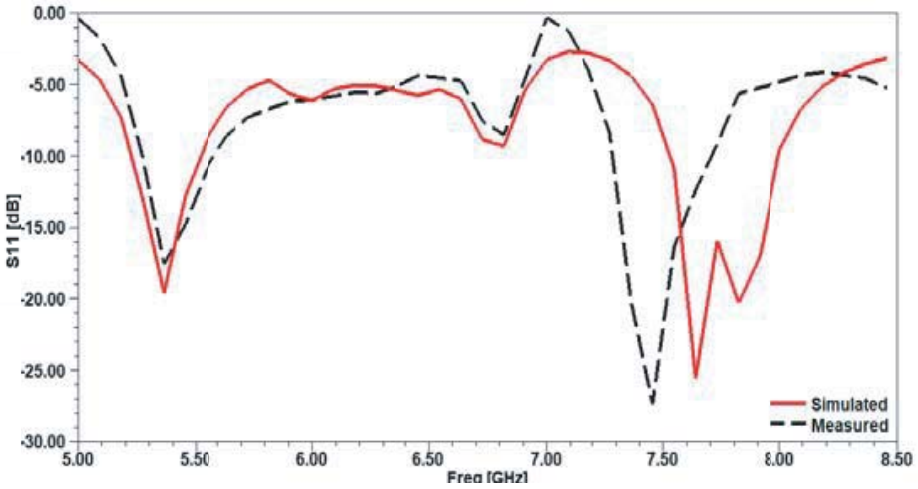

Figure 16. Simulated and measured S_{11} and axial for design 3.

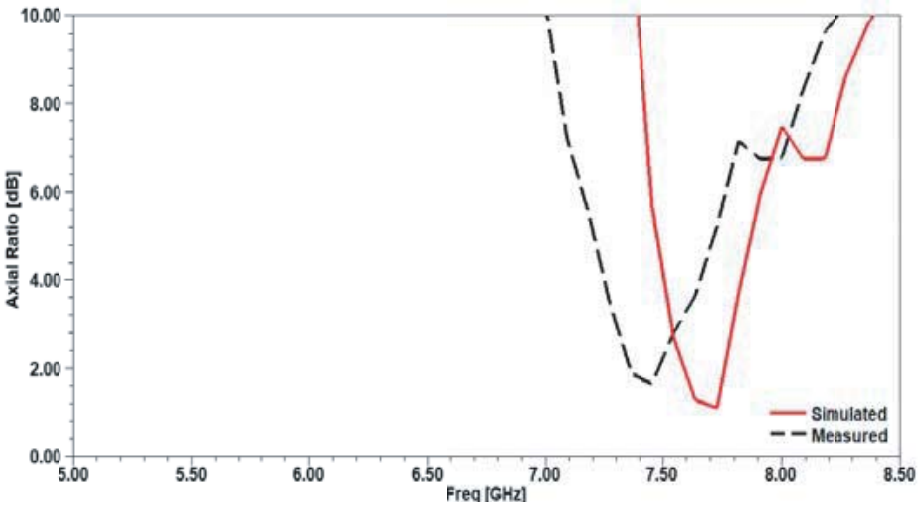

Figure 17. Simulated and measured axial ratio.

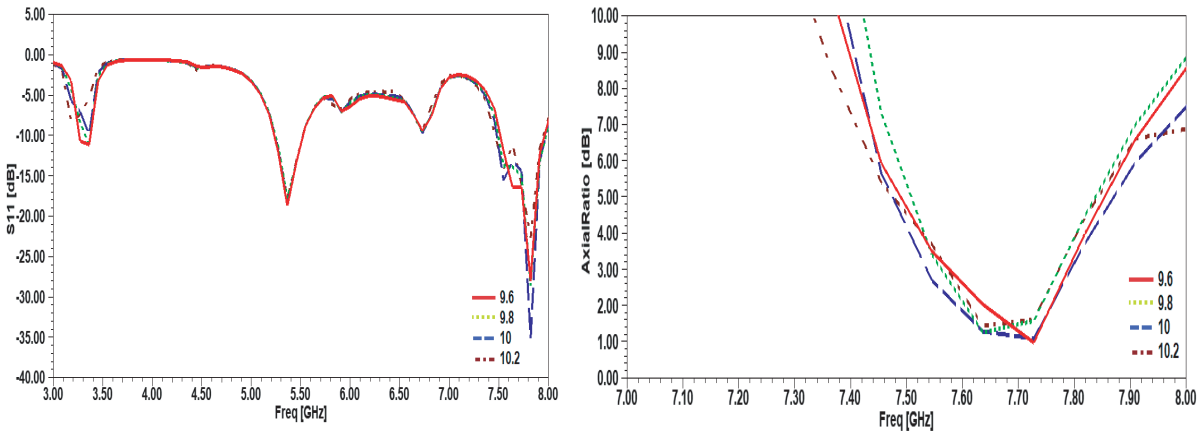

(a) (b)

Figure 18. (a) S_{11} vs frequency for various cross slot length. (b) Axial ratio vs frequency for various cross slot length.

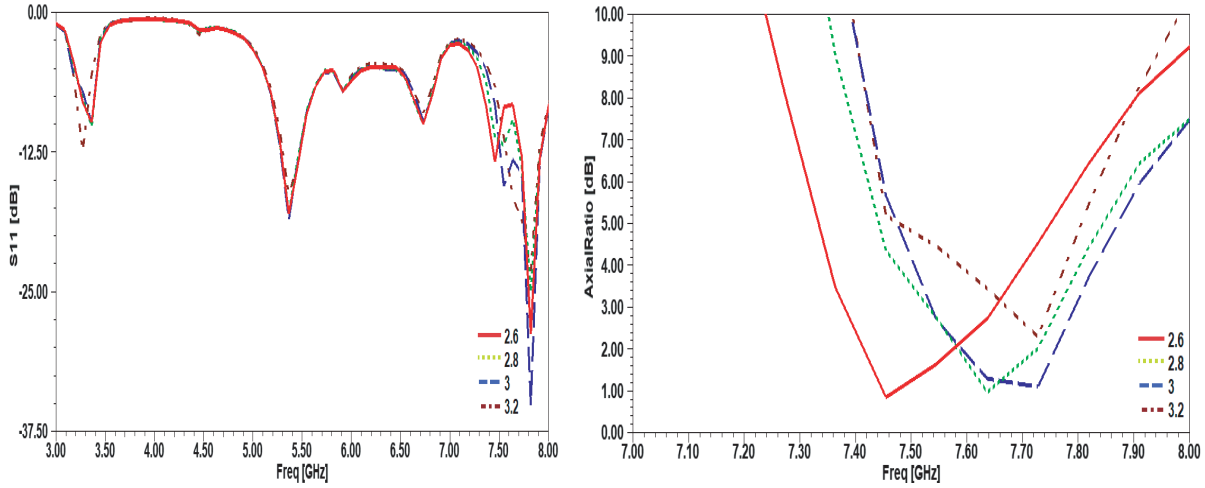

(a) (b)

Figure 19. (a) S_{11} vs frequency for various cross slot width. (b) Axial ratio vs frequency for various cross slot width.

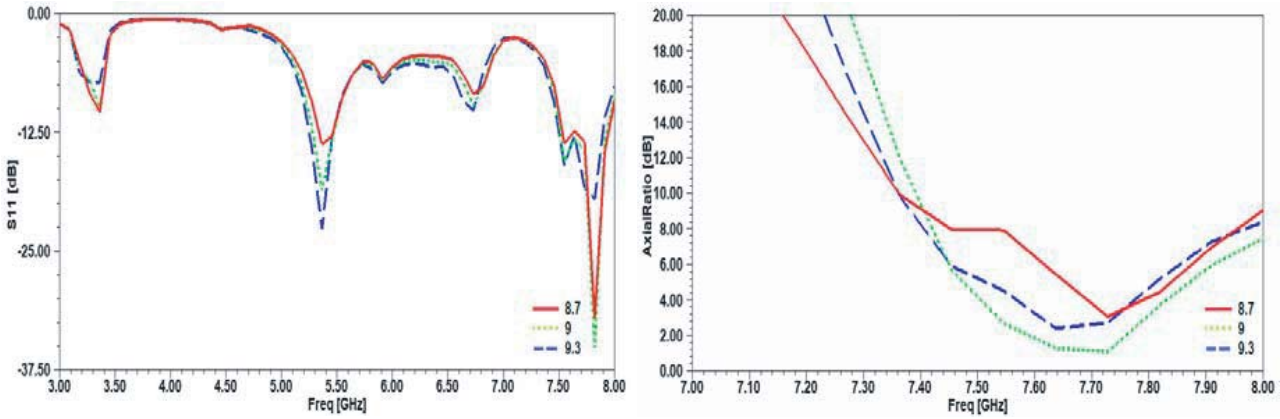

(a) (b)

Figure 20. (a) S_{11} vs frequency for various aperture slot length. (b) Axial ratio vs frequency for various aperture slot length.

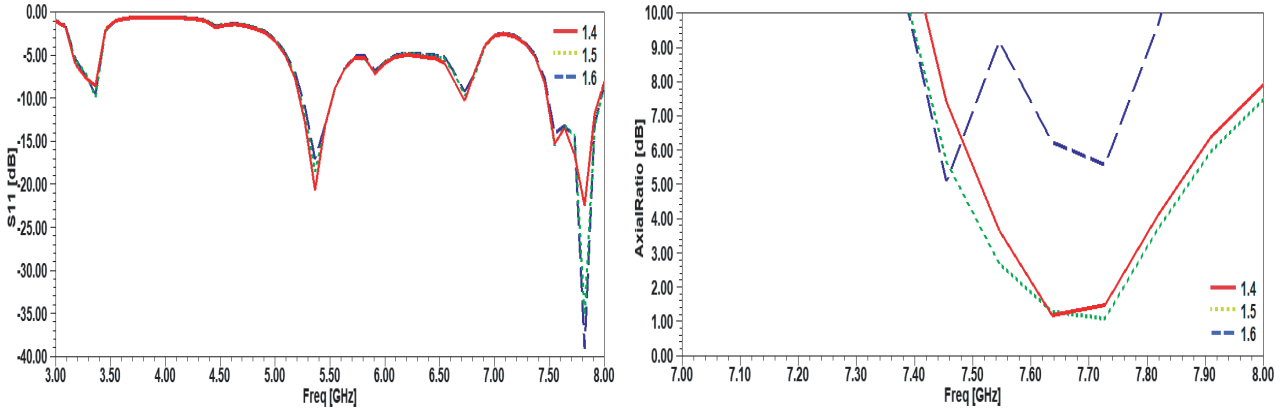

(a) (b)

Figure 21. (a) S_{11} vs frequency for various aperture slot width. (b) Axial ratio vs frequency for various aperture slot width.

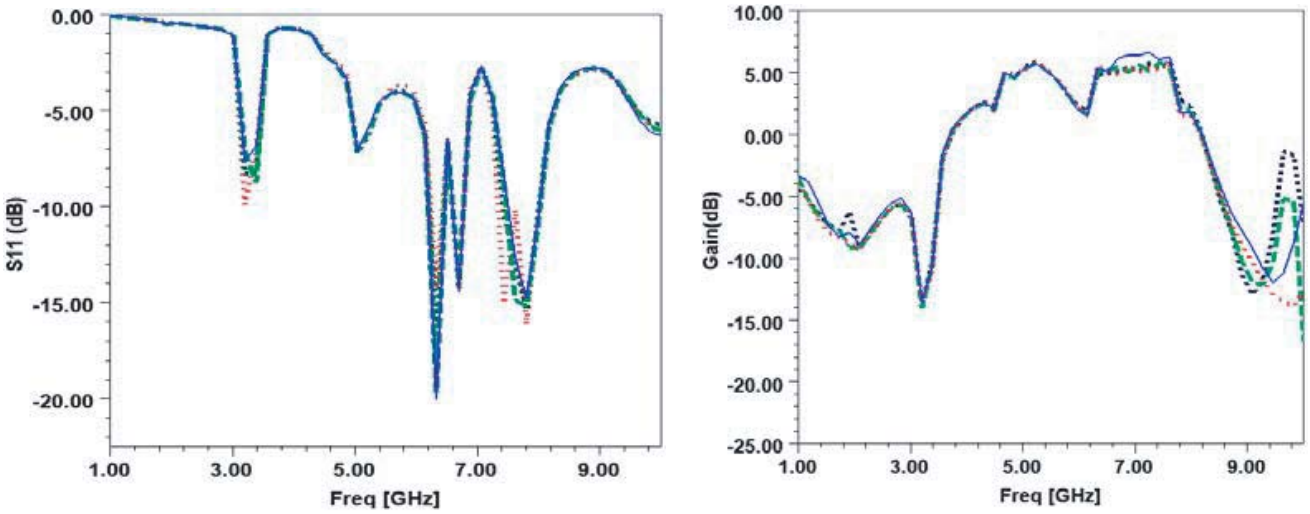

Figure 22. (a) S_{11} vs frequency. (b) Gain vs frequency: for varying height of 6th stacked layer height in 6 layers geometry.

7. CONCLUSION

A layout using novel materials, i.e., anisotropic material and isotropic material stacked alternatively to form a four-layer stack structure with aperture coupled feed process for excitation, has been employed. The orthogonal mode pair $TE^{x}_{\delta 21}$ and $TE^{y}_{2\delta 1}$ has been excited at frequencies 7.54 GHz and 7.8 GHz respectively in YZ and XZ planes to deliver circular polarization. A circularly polarized bandwidth in the region (7.54 GHz–7.92 GHz) in combination with impedance bandwidth in the region (5.23 GHz–5.52 GHz) has been accomplished. A gain of 5.2 dBi has been attained. The proposed antenna is excellent for the C band and weather radar application.

REFERENCES

1. Gotra, S., G. Varshney, R. S. Yaduvanshi, and V. S. Pandey, "Dual-band circular polarisation generation technique with the miniaturization of a rectangular dielectric resonator antenna," *IET Microwaves, Antennas & Propagation*, Vol. 13, No. 10, 1742–1748, 2019.
2. Varshney, G., R. Singh, V. S. Pandey, and R. S. Yaduvanshi, "Circularly polarized two-port MIMO dielectric resonator antenna," *Progress In Electromagnetics Research M*, Vol. 91, 19–28, 2020.
3. Varshney, G., "Gain and bandwidth enhancement of a singly-fed circularly polarised dielectric resonator antenna," *IET Microwaves, Antennas & Propagation*, Vol. 14, No. 12, 1323–1330, 2020.
4. Ngan, H. S., X. S. Fang, and K. W. Leung, "Design of dual-band circularly polarized dielectric resonator antenna using a higher-order mode," *2012 IEEE-APS Topical Conference on Antennas and Propagation in Wireless Communications (APWC)*, 424–427, Cape Town, 2012.
5. Pan, Y. and K. W. Leung, "Wideband circularly polarized trapezoidal dielectric resonator antenna," *IEEE Antennas and Wireless Propagation Letters*, Vol. 9, 588–591, 2010.
6. Ding, Y., K. W. Leung, and K. M. Luk, "Compact circularly polarized dualband zonal-slot/DRA hybrid antenna without external ground plane," *IEEE Transactions on Antennas and Propagation*, Vol. 59, No. 6, 2404–2409, Jun. 2011.
7. Gupta, R. and A. Vaish, "Deminiaturized mode control rectangular dielectric resonator antenna," *Progress In Electromagnetics Research M*, Vol. 86, 173–182, 2016.
8. Gupta, A. and R. K. Gangwar, "Dual-band circularly polarized aperture coupled rectangular dielectric resonator antenna for wireless applications," *IEEE Access*, Vol. 6, 11388–11396, 2018.

9. Khalajmehrabadi, A., M. K. A. Rahim, and M. Khalily, "Dual band double stacked dielectric resonator antenna with a P-shape parasitic strip for circular polarization," *2011 IEEE International RF & Microwave Conference*, 444–447, Seremban, Negeri Sembilan, 2011.
10. Fakhte, S., H. Oraizi, and R. Karimian, "A novel low-cost circularly polarized rotated stacked dielectric resonator antenna," *IEEE Antennas and Wireless Propagation Letters*, Vol. 13, 722–725, 2014.
11. Varshney, G., S. Gotra, R. Singh, V. S. Pandey, and R. S. Yaduvanshi, "Dimensions selection criteria of stair-shaped slot for obtaining the wideband response of CPDRA," *Def. Sci. J.*, Vol. 69, No. 5, 442–447, 2019.
12. Pan, Y. M. and K. W. Leung, "Wideband omnidirectional circularly polarized dielectric resonator antenna with parasitic strips," *IEEE Transactions on Antennas and Propagation*, Vol. 60, No. 6, 2992–2997, Jun. 2012.
13. Wang, K. X. and H. Wong, "A circularly polarized antenna by using rotated-stair dielectric resonator," *IEEE Antennas and Wireless Propagation Letters*, Vol. 14, 787–790, 2015.
14. Dick, G. J. and J. Saunders, "Measurement and analysis of a microwave oscillator stabilized by a sapphire dielectric ring resonator for ultra-low noise," *IEEE Transactions on Ultrasonics, Ferroelectrics, and Frequency Control*, Vol. 37, No. 5, 339–346, Sept. 1990.
15. Zhang, M., B. Li, and X. Lv, "Cross-slot-coupled wide dual-band circularly polarized rectangular dielectric resonator antenna," *IEEE Antennas and Wireless Propagation Letters*, Vol. 13, 532–535, 2014.
16. Gupta, R., G. Bakshi, and A. Bansal, "Dual-band circularly polarized stacked sapphire and TMM13i rectangular DRA," *Progress In Electromagnetics Research M*, Vol. 91, 143–153, 2020.
17. Giles, J., S. K. Jones, D. G. Blair, and M. J. Buckingham, "A high stability microwave oscillator based on a sapphire loaded superconducting cavity," *Proceedings of the 43rd Annual Symposium on Frequency Control*, 89–99, Denver, CO, USA, 1989.
18. Seo, D. C. and Y. Sung, "Stacked open-loop square ring antenna for circular polarization operation," *IEEE Antennas and Wireless Propagation Letters*, Vol. 14, 835–838, 2015.
19. Varshney, G., V. S. Pandey, and R. S. Yaduvanshi, "Dual-band fan-blade-shaped circularly polarised dielectric resonator antenna," *IET Microwaves, Antennas & Propagation*, Vol. 11, No. 13, 1868–1871, 2017.
20. Kumar, R., G. Varshney, R. S. Yaduvanshi, D. K. Dwivedi, and V. S. Pandey, "Dual-band dielectric resonator antenna with multi-frequency circular polarisation," *IET Microwaves, Antennas & Propagation*, Vol. 14, No. 5, 435–439, 2020.
21. Varshney, G., S. Gotra, J. Kaur, V. S. Pandey, and R. S. Yaduvanshi, "Obtaining the circular polarization in a nano-dielectric resonator antenna for photonics applications," *Semiconductor Science and Technology*, Vol. 34, No. 7, 07LT01, 2019.